Ultrasound in gas–liquid systems: Effects on solubility and mass transfer

F. Laugier, C. Andriantsiferana, A.M. Wilhelm *, H. Delmas

Laboratoire de Génie Chimique, 5 rue Paulin Talabot, BP 1301, 31 106 Toulouse, France

ABSTRACT

The effect of ultrasound on the pseudo-solubility of nitrogen in water and on gas–liquid mass transfer kinetics has been investigated in an autoclave reactor equipped with a gas induced impeller. In order to use organic liquids and to investigate the effect of pressure, gas–liquid mass transfer coefficient was calculated from the evolution of autoclave pressure during gas absorption to avoid any side-effects of ultrasound on the concentrations measurements.

Ultrasound effect on the apparent solubility is very low (below 12%). Conversely ultrasound greatly improves gas–liquid mass transfer, especially below gas induction speed, this improvement being boosted by pressure. In typical conditions of organic synthesis: 323 K, 1100 rpm, 10 bar, $k_L \cdot a$ is multiplied by 11 with ultrasound (20 kHz/62.6 W).

The impact of sonication is much higher on gassing out than on gassing in. In the same conditions, this enhancement is at least five times higher for degassing.

1. Introduction

Power ultrasound is known to enhance some multiphase chemical reactions, by affecting the yield of the reaction and/or its selectivity [1], but this effect at 20 kHz being mainly mechanical, concerns mostly interfacial transfer kinetics. Whereas the positive effect of ultrasound is well-known on solid surface as a result of the most developed ultrasound application: solid cleaning and in liquid–liquid reactions by generating very fine emulsions [1], its effect on gas–liquid systems is not clear.

Few papers are devoted to, or even mention, gas–liquid mass transfer with ultrasound. Some elements can be found in the fields of biotechnology and wastewater treatment. In his review on sonobioreactors, Chisti [2] attributed part of the beneficial effects of ultrasound in biotechnology to mass transfer improvements: increased mass transfer around the cells (improving the exchanges of nutrients and products), but also inside the cells (thanks to micro-streaming) [3,4]; this enhancement of mass transfer is also beneficial to the feed of oxygen, to the removal of carbon dioxide, and to the dissolution of solid nutrients in bioreactors.

In the field of wastewater treatment by sonochemistry, Weavers and Hoffmann [5] and Zhang et al. [6] have also suggested that possible mass transfer steps could be altered by ultrasound. For instance, in sono-ozonation, the steps are numerous: absorp-tion of ozone to the solution, degradation of ozone to radicals, and degassing of ozone. Weavers and Hoffmann [5] tried to decouple these phenomena by using different reactors configurations: open, closed, and sparged, and showed that the main effect of ultrasound was to increase the degradation of ozone, and consequently mass transfer through the concentration gradient and not through the mass transfer coefficient. Zhang et al. [6] carried out transient absorption and desorption experiments, with or without injection of gas, and showed an increase in the kinetics of degassing of oxygen (by 6–20) linked to the emitted power, and a major effect of ultrasound on the kinetics of degradation of ozone. But they calculated low values of Hatta numbers, proving that no acceleration of absorption could occur through the chemical degradation of ozone. Adewuyi [7], in his review on hybrid advanced oxidation processes for wastewater treatment, concluded by the importance of the effects of ultrasound on ozone mass transfer, mostly in large-scale reactors, and stressed the need for such studies.

Kumar et al. [8] investigated gas–liquid mass transfer with a 20 kHz ultrasonic horn (13 mm) and a gas sparger; they concluded that the distance horn-sparger was crucial for the gas bubbles to be injected in the active cavitation zone. Low frequency (20 kHz) appeared more favorable than high frequency (500 kHz). They allotted the observed enhancement of mass transfer to a reduction of gas bubble size.

The treatment of VOC by ultrasound and stripping was investigated by Ayyildiz et al. [9] with two types of sparger. They show a

synergistic effect of these two processes, and explained the role of ultrasound by an increase of gas holdup, whereas the size of bubbles measured by a camera, stayed unchanged. Then they tried to model this effect [10] during the degradation of VOC, and stressed that volatility was much more altered by ultrasound than diffusivity in the liquid (mostly for low volatility compounds).

Indeed, mass transfer kinetics improvement is not the only effect of ultrasound, solubility has been also found to be reduced [11,12]. In a 500 kHz (0–100 W) ultrasonic reactor (0.2–0.6 L), Gondrexon et al. [11] report that this pseudo-solubility is independent of sonicated volume and ultrasonic power, and that the equilibrium of dissolved gas concentration reached under sonication results from the competition between desorption induced by cavitation bubbles and absorption caused by the formation of an 'acoustic fountain' at the free surface of the liquid. This effect of degassing has been very used in industry for molten metals and polymers, as shown by the high number of patents on degassing.

The purpose of this study is to investigate gas–liquid mass transfer in ultrasonically irradiated systems. In view of applications of ultrasound to multiphase reactions involving high pressure and temperature, an ultrasonic autoclave reactor with controlled mechanical agitation was designed and implemented. In order to use any kind of liquid and to avoid side-effects of ultrasound on concentration measurements, solubility and mass transfer coefficient have been calculated from the pressure measurements in closed system. The effects of pressure and temperature on solubility and mass transfer rate have been investigated for gassing in and gassing out processes with ultrasound and/or mechanical stirring.

2. Experimental

2.1. Experimental set-up

The experimental set-up is presented in Fig. 1. All experiments were carried out in a 1 l stainless steel ultrasonic autoclave reactor (1) (1–12 bara) fitted with a gas inducing 6 blades turbine (2′) (Dispermax), with an adjustable stirring speed up to 3000(±1) rpm (2). This gas induced impeller is made of two distinct parts:

- A hollow axis with a hole (a), where gas is sucked in.
- A Rushton-like 6 blades turbine screwed to the axis, with holes (b) behind the blades to throw out the gas sucked in at the top of the axis.

Gas is induced only if low pressure at the exit holes (b) is below the static pressure at the depth of the holes. This low pressure is caused by rotation of the impeller, so gas induction needs a critical speed to take place.

Ultrasound is emitted by a 20 kHz cup-horn (3) (35 mm ultrasonic probe: Sinaptec PLANUS P2035041), with a power input of 200 W (generator: Sinaptec NEXUS 198-NC600) and cooled with compressed air (4). The reactor is connected, via a pressure reducer (1–12 bara), to a gas tank (5) which can be fed by nitrogen supply network (11 bara) or by a cylinder of gas (6). Temperature of the liquid in the reactor (T_1 = 298–368 K) is monitored via a heating shell (7) and a cooling coil (8) with cold water, with an accuracy of ±1 K. Temperature (T_1) and pressure in the reactor (P_1) and in the tank (P_2) are recorded thanks to a PC. The fast pressure probe in the reactor (P_1) has an adjustable scale between 1 and 20 bara and an accuracy ±0.005 bar in the actual operating conditions. Samples can be collected via a tube and a valve (9).

Designed for organic synthesis involving harmful reagents (as: $CO–H_2$ mixture for hydroformylation), the reactor had to be completely safe. So the reactor has been located in a polycarbonate gloves box, equipped with gas detectors, safety valves and a powerful fume hood. In any case of emergency like the breakdown of cooling water/air supplies or fume hood, overheating of the reactor/shell (T_2), or any failure of gas detection, the electric power supply is shut off, while an alarm is set on. And in case of electricity failure, automatic valves close the reservoir, and open the by-pass for cooling water.

2.2. Power consumption

An estimation of power dissipated by mixing or sonication has been done beforehand beginning experiments:

2.2.1. Ultrasonic power dissipated in the liquid (P_{us})
Acoustic power dissipated in the liquid (P_{us} in W) has been related to the power percentage indicated on ultrasonic generator ($P\%_{us}$ in %) by way of the well-known calorimetric method. This calorimetric study is based on the temperature increase of a known quantity of water (500 g) placed in the reactor (thermally insulated) during the first 500s of sonication ($P\%_{us}$ fixed).

The relationship obtained is

$$P_{us} = 0.626 P\%_{us} \tag{1}$$

So, when generator is set at $P\%_{us}$ = 100% the power received by the liquid is equal to 62.6 W. Experiments carried out at various pressures showed that this relationship is not depending on pressure in the study range.

2.2.2. Power dissipated by stirrer (P_N)
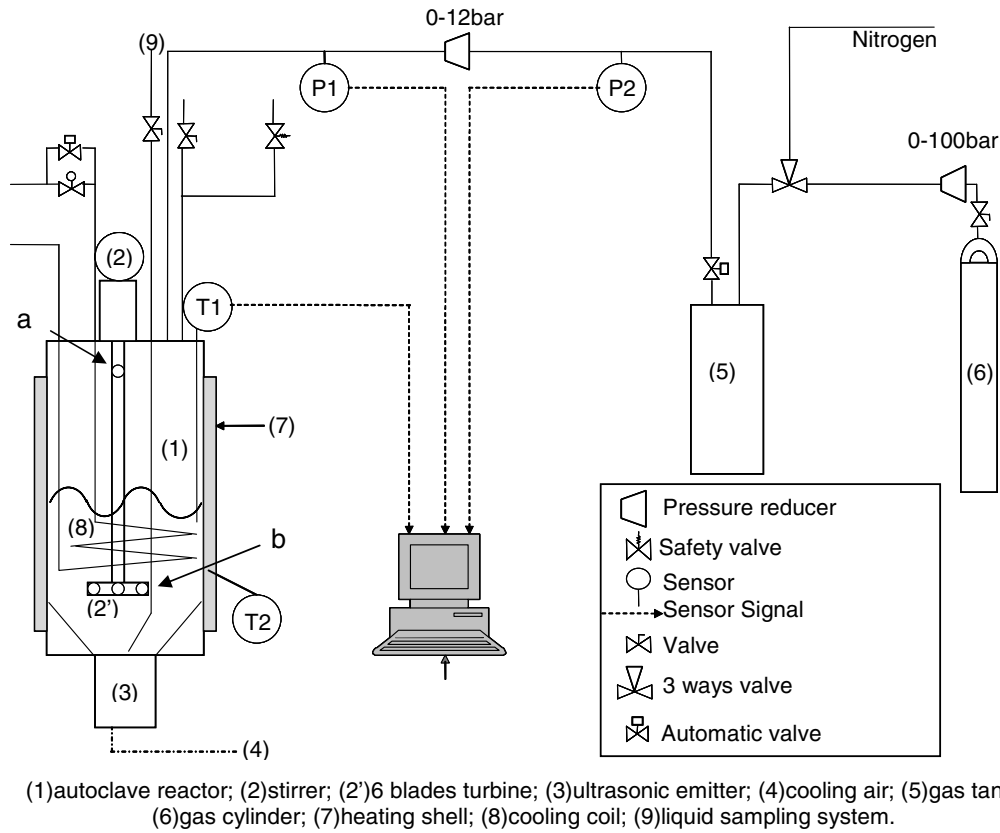At any mixing speed above 300 rpm, Reynolds number is over 2000, which assesses that flow is turbulent.

(1)autoclave reactor; (2)stirrer; (2')6 blades turbine; (3)ultrasonic emitter; (4)cooling air; (5)gas tank; (6)gas cylinder; (7)heating shell; (8)cooling coil; (9)liquid sampling system.

Fig. 1. Experimental set-up.

Power dissipated by a mixing blade (P_N) depends on its diameter D in m, the mixing speed N in round/s, liquid density ρ in kg/m^3 and of a dimensionless number called power number N_P, which is constant in turbulent flow [13]

$$P_N = N_P \cdot \rho \cdot N^3 \cdot D^5 \tag{2}$$

The power number of the present gas induced blade is here approximated to the power number of Rushton blades: 5.5, but gas induction is known to reduce the power number [13]. So the mixing power calculated by this equation is an over-estimation. Anyway this power is always much lower than dissipated acoustic power (Table 1).

Anyway the maximum power dissipated by stirrer (16.7 W at 3000 rpm) is the quarter of the maximum ultrasonic power received by the system when ultrasound is set at 100% (62.6 W). Almost the same ratio is observed using a direct measurement method: Wattmeter. Ultrasound set at 100% consume 230 W, whereas mixer at 3000 rpm consumes 63 W, so electrical consumption of ultrasound is 3.65 times higher than electrical power consumed by stirrer.

2.3. Experiments procedure

The gas–liquid system chosen was nitrogen and deionised water.

Those procedures are known as dynamic pressure-step method and are routinely used in autoclave reactors.

This experimental set-up is fitted to study gas absorption as well as desorption. For both phenomena, the first steps are the same:

- Fill reactor with 700 g of water and tightly close it.
- Strip out oxygen from water thanks to a moderate flux of nitrogen and vigorous stirring at atmospheric pressure.
- Nitrogen flux and stirring are stopped, gas outlet is closed.

Then procedures are different for absorption and desorption.

2.3.1. Absorption experiments (gassing in)

The pressure is kept at 1 bara and with a vigorous stirring (>2000 rpm), water is saturated with nitrogen (P_0). Stirring is stopped, recording is started, and reactor is filled at 11 bara of nitrogen. After pressure stabilization (Fig. 2, Phase 1, curve: 1600 rpm, P_m), stirring is started again (Fig. 2, t_0) at desired study speed and gas absorption occurs (Fig. 2, phase 2). The end of gas absorption is reached when pressure in reactor is constant (Fig. 2, Phase 2, 1600 rpm, P_f).

To study the influence of ultrasound on final pressure and so to infer the impact of sonication on dissolved gas concentration,

Table 1
Effects of ultrasound on solubility

| N (rpm)	P_N (W)	T (K)	$P\%_{us}$ (%)	P_{us} (W)	P (bara)	C_{us}/C^* (%)
300	0.02	298	100	62.6	10.91	94.9
500	0.08	298	100	62.6	10.91	94.4
700	0.21	298	100	62.6	2.91	88.6
700	0.21	298	100	62.6	3.76	89.4
700	0.21	298	100	62.6	5.92	89.7
700	0.21	298	100	62.6	8.50	90.3
700	0.21	298	100	62.6	10.70	91.2
800	0.32	298	100	62.6	10.69	97.3
1100	0.82	298	100	62.6	10.70	96.0
1100	0.82	323	100	62.6	10.72	94.4
1100	0.82	298	50	31.3	10.50	100.0
1600	2.53	298	100	62.6	10.80	97.2
1600	2.53	298	50	31.3	10.60	100.0
2000	4.95	298	100	62.6	XXX	100.0
3000	16.71	298	100	62.6	XXX	100.0
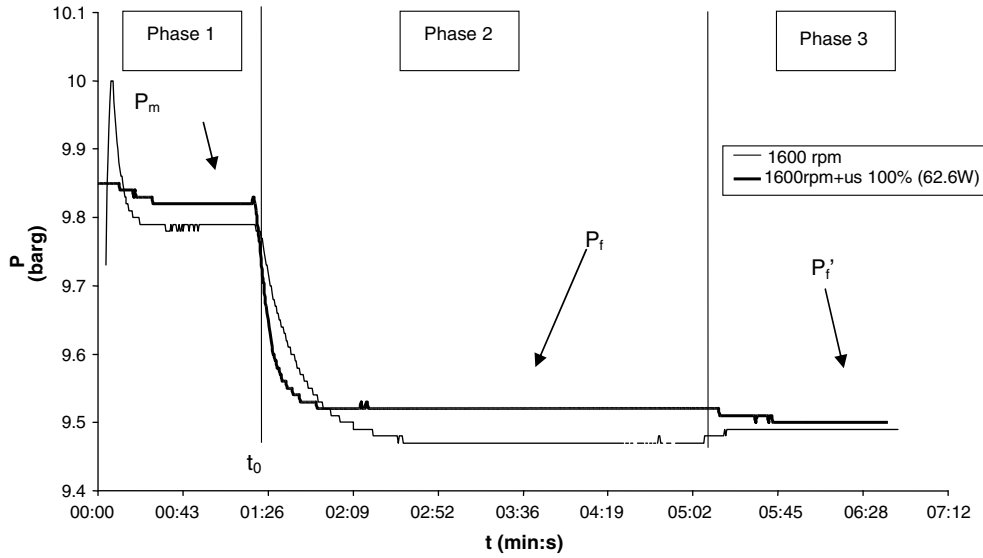
Fig. 2. Typical pressure (in barg) curve during absorption experiments, at 298 K.
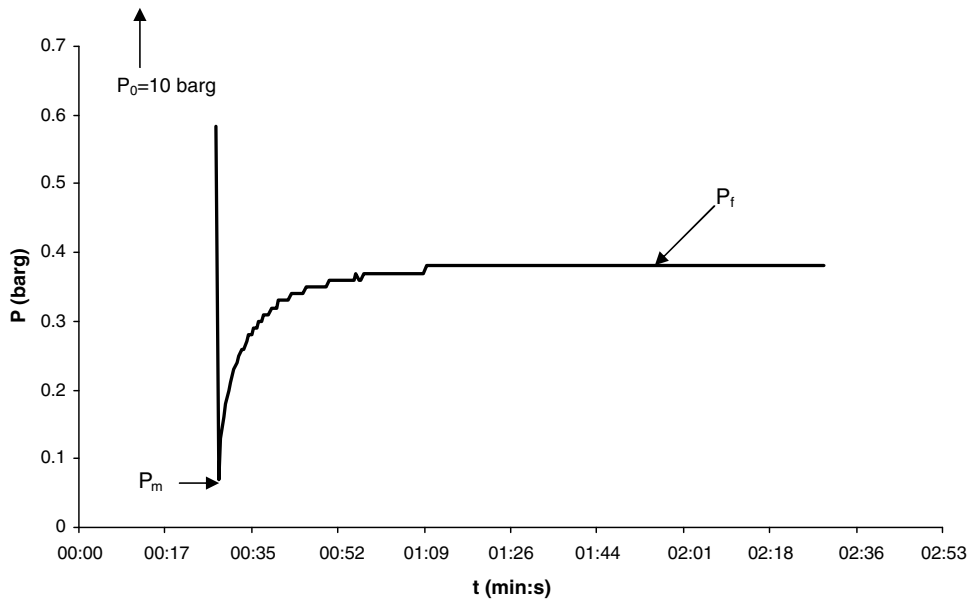

Fig. 3. Typical pressure (in barg) curve during desorption experiments, at 2000 rpm, 298 K.

ultrasonic generator is set on (Fig. 2, Phase 3, curve: 1600 rpm, P_f').

Ultrasound can also be emitted during absorption; in this case, after stabilization period (Fig. 2, Phase 1, 1600 rpm + us100%(62 W), P_m), ultrasound and stirrer are started simultaneously (Fig. 2, t_0). When pressure is steady (Fig. 2, curve: 1600 rpm + us100%(62 W), P_f) dynamic equilibrium obtained under sonication is reached. Then, ultrasound is stopped to reach solubility (Fig. 2, Phase 3, curve: 1600 rpm + us100%(62W), P_f').

2.3.2. Desorption experiments (gassing out)

The reactor is filled with 11 bara of nitrogen, vigorous mixing (>2000 rpm) is kept during 10 min (Experiments have shown that solubility with stirrer speed above 1600 rpm is reached in less than 5 min).

Stirrer is stopped, recording is started, reactor outlet is opened; reactor is purged down to atmospheric pressure (P_m) and closed as

quickly as possible (Fig. 3), stirrer and/or ultrasound is/are started. Desorption is finished when pressure is steady (P_f).

3. Solubility

Nitrogen can be considered as a perfect gas in the low pressure range investigated here. Solubility at final pressure ($C_l^*(P_f)$) can easily be deduced from the total amount of nitrogen transferred to the liquid and the initial concentration of dissolved gas (C_l^{*0} at initial sure P_0) thanks to the following expression:

$$C_l^*(P_f) = \frac{\Delta P \cdot V_g}{R \cdot T_1 \cdot V_l} + C_l^{*0} \tag{3}$$

Ultrasound is known to decrease thermodynamic static equilibrium (solubility) C_l^* to a dynamic equilibrium C_{lUS}^* [11,12], also calculated with Eq. (3). For fixed temperature and pressure solubility is reached at different delay times depending on the meth-

od used, but its value is constant C_I^*, whereas C_{US} depends on C_{IUS}^*.

It can be noticed that C_I^{*0} is highly dependant on the value of Henry law constant (H). So a calculation loop has been implemented to calculate the experimental H value from data without ultrasound. The results are in good agreement with values reported in handbooks (±5%).

Experiments carried out simultaneously with ultrasound and mechanical stirring, yield the same results as those where ultrasound is set on only after an absorption process with mixing as shown in Fig. 2. We can clearly see that total pressure difference reached by curves is equal, but be careful to compare the same state of equilibrium, so systems in the same state. For instance, if we want to compare solubility (pressure difference: ΔP): for the curve without sonication (Fig. 2, 1600 rpm) $\Delta P = P_m - P_f = 0.32$, whereas for the experiment which began with ultrasound $\Delta P = P_m - P_f = 0.33$. There is no effect of the procedure on the equilibrium reached. Main results are presented in Table 1, each value being the average of at least 3 experiments, for the temperature effect at 1100 rpm each of the 3 points is the result of 10 experiments driven in the same conditions. In Table 1 XXX means that at 2000–3000 rpm, no effect of sonication has been observed at any pressure ranging from 3 to 11 bara.

The influences of pressure and temperature are very weak in the range of operating conditions. A raise of 25 K in temperature (at 1100 rpm) increases the effects of sonication by 1.6%. For pressure it is the opposite, increasing pressure results in a reduction of ultrasonic effects on solubility (2.6% lost between 2.91 and 10.70 bara).

The relative difference between solubility and pseudo-solubility is reported in literature [12] to be around 20–30% in air–water system at atmospheric pressure. In this study, the difference stays always below 12%. Kapustina [12] also denoted that diminishing pressure from 1 to 0.5 bara decreased the ratio C_{us}/C^* from 70% to 30%. We can suppose that this effect still affect dissolved gas concentration above atmospheric pressure, what would explain the negative effect of pressure on pseudo-equilibrium.

By measuring dissolved oxygen concentration, Gondrexon et al. [11] have shown in their study of degassing in high frequency sonochemical reactors that dynamic equilibrium obtained under sonication results from a competition between degassing action of ultrasound resulting from cavitation bubbles and regassing action caused by the formation of an acoustic fountain enhancing the uptake of oxygen from atmosphere and that this dynamic equilibrium depends on the ultrasonic power dissipated in the liquid.

In their study Gondrexon et al. [11] used a reflector at the surface of the liquid to limit adsorption caused by acoustic fountain, so they observed a diminution in dissolved gas concentration and concluded that degassing effect was a competition between degassing and regassing. Since wave frequency here is only 20 kHz the acoustic fountain does not take place in this study, on the contrary in the present study we improved regassing effect with a gas induced impeller to confirm Gondrexon observations.

The solubility ratio in Table 1 shows a minimum versus stirrer speed, at $N = 700$ rpm, just before the critical speed (see details in Section 4.1). At high stirrer speed (>2000 rpm) this solubility ratio tends to 1. At intermediate stirrer speed (1100 and 1600 rpm) when power is divided by 2, effects of ultrasound on solubility disappear.

Those observations confirm the competition between gassing in, due to gas induction, and gassing out caused by cavitation. At high stirrer speed (presence of gas induction) or low sonication power, gas–liquid mass transfer overcomes ultrasound gassing out effects. The effect of ultrasound on solubility is maximum at: low pressure, high temperature, high sonication power and low stirrer speed.

4. Mass transfer

This paragraph presents mostly the results of the absorption experiments (4.1–4.3). Data concerning gassing out will only be discussed in the last Section 4.4.

Due to the low solubility of nitrogen in water, mass transfer resistance is supposed to be located in the liquid film. Thanks to this assumption, the following logarithmic equation [14] can be written to calculate mass transfer coefficient as a function of time and pressure:

$$\ln\left(\frac{P_m - P_f}{P_{(t)} - P_f}\right) = \left(\frac{P_m - P_0}{P_f - P_0}\right) \cdot k_L \cdot a \cdot (t - t_0) \tag{4}$$

where $k_L \cdot a (s^{-1})$ is the global mass transfer coefficient. To obtain $k_L \cdot a$, the logarithmic expression of instantaneous pressure in Eq. (4) was plotted versus time between 20 and 70% of the overall pressure loss of the experiment (straight part of the pressure curve). $k_L \cdot a$ is directly obtained from the slope of this curve divided by the pressure constant $\left(\frac{P_m - P_0}{P_f - P_0}\right)$.
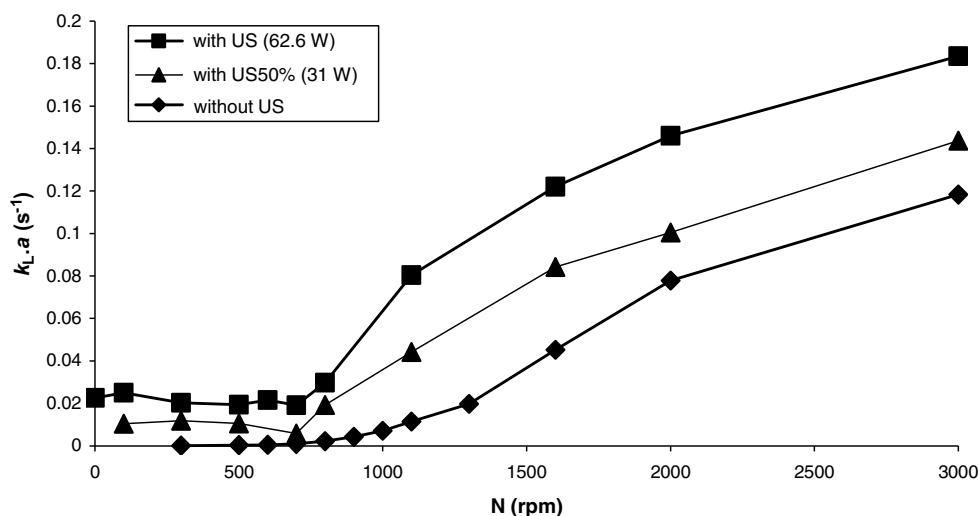

Fig. 4. Effect of stirrer speed (N) on mass transfer coefficient ($k_L \cdot a$) Standard scale.

4.1. Influence of stirrer speed

Gas induction requires a critical impeller speed [14–16], this threshold being mainly dependant on the liquid density, the geometry of the studied system and the height of liquid above impeller at rest. Fig. 4 clearly shows that this threshold value is between 700 and 800 rpm. Without ultrasound, effect of stirring speed on $k_L \cdot a$ is higher: mass transfer continuously increases with mixing speed, even below the critical impeller speed (Fig. 5) as reported in previous publications [14–16]. With ultrasound, mass transfer coefficient due to cavitation is constant below the critical speed and is highly enhanced – up to hundredfold-compared to silent conditions. Above the critical speed, $k_L \cdot a$ increases with stirrer speed and is still enhanced compared to silent conditions, mainly because cavitation splits bubbles thus improving interfacial area and thus mass transfer.

This enhancement of gas–liquid mass transfer by ultrasound is, as expected, related to the power delivered to the ultrasonic emitter [8] as shown in Fig. 5.

4.2. Influence of pressure

As expected [17,18], pressure (Fig. 6) has no significant influence on global mass transfer coefficient in silent conditions. On the other hand, with ultrasound influence of pressure becomes larger (Fig. 6): at 9 bara and 1100 rpm (in presence of gas induction), $k_L \cdot a$ with ultrasound is 8 times more than the one in silent condition, whereas at 3 bara the factor is only 3. At 700 rpm (without gas induction) while no significant ultrasound effect is found under 4 bara, a strong enhancement is performed at higher pressure 10.5 bara ultrasound multiplies mass transfer coefficient by more than 20.
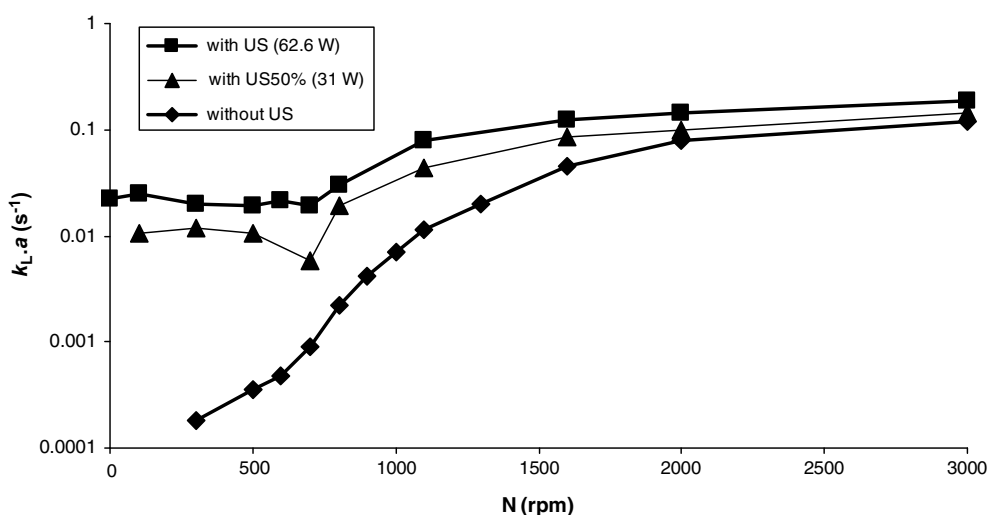

Fig. 5. Effect of stirrer speed (N) on mass transfer coefficient ($k_L \cdot a$) logarithmic scale.
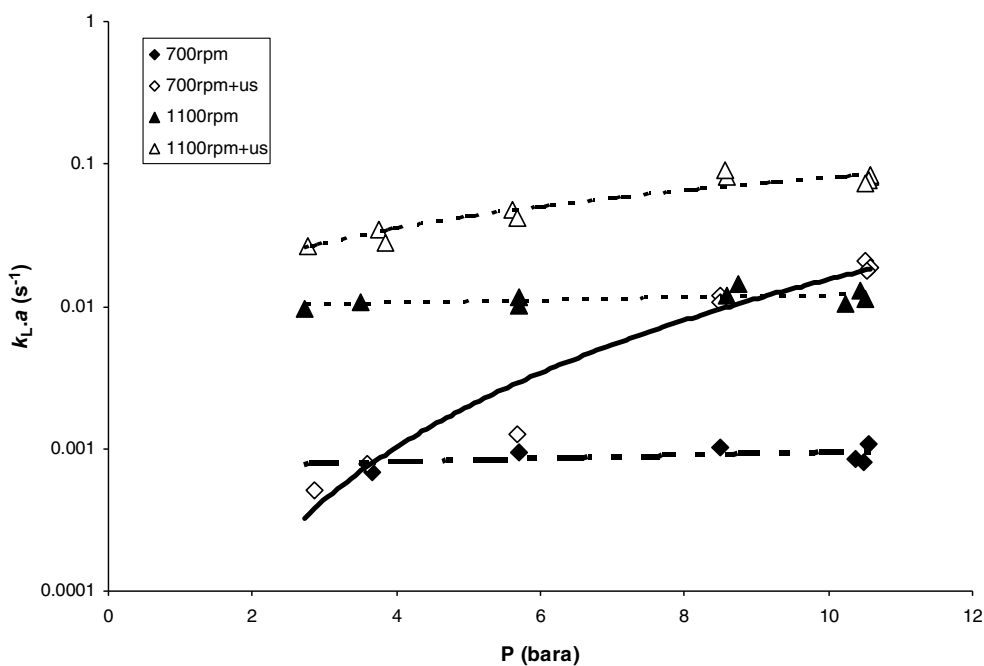

Fig. 6. Effect of pressure on mass transfer at 298 K.

The same trend has been observed at 323 K. It can be connected to the positive effect of pressure on cavitation, at increased pressures, cavitation threshold is higher but the effects are more violent [19].

4.3. Influence of temperature

Similar to the case of pressure, temperature in silent condition does not show any significant influence on mass transfer (Fig. 7). Application of ultrasound together with stirring provides an improvement on mass transfer in the temperature range applied, depending on impeller speed. Below the critical speed (700 rpm), an increase in temperature decreases slightly $k_L \cdot a$ under sonication as expected [20], whereas in silent conditions heating results in a small increase of $k_L \cdot a$. So at 700 rpm the ultrasonic mass transfer enhancement, still very high, is divided by 4 when increasing temperature from 298 to 368 K.

In conditions of gas induction (1100 rpm) the ultrasonic beneficial effect on mass transfer is not depending of the temperature:

sonication always multiplies $k_L \cdot a$ by about seven. It has to be noticed that noticed in presence of gas induction, mass transfer with ultrasound follows closely the trend observed in silent conditions (Figs. 5 and 7). This suggests that ultrasonic improvement in those conditions is mainly due to the breakage of bubbles generated by gas induction, which results in an increase of interfacial area (a) and consequently of mass transfer.

4.4. Comparison of kinetics of gassing in and gassing out

In Fig. 8 are compared global mass transfer coefficients for absorption and desorption experiments, with or without ultrasound. It is obvious that the fastest mass transfer is obtained for desorption experiments under sonication (void squares). For instance, the gassing out $k_L \cdot a$ is multiplied by 5 when sonication is added to vigorous mechanical stirring (N = 2000 rpm) and by 400 when US is compared to no stirring (N = 0 rpm). Moreover, it can be noticed that desorption mass transfer coefficient with ultrasound (void squares) is not influenced by mixing velocity: at any
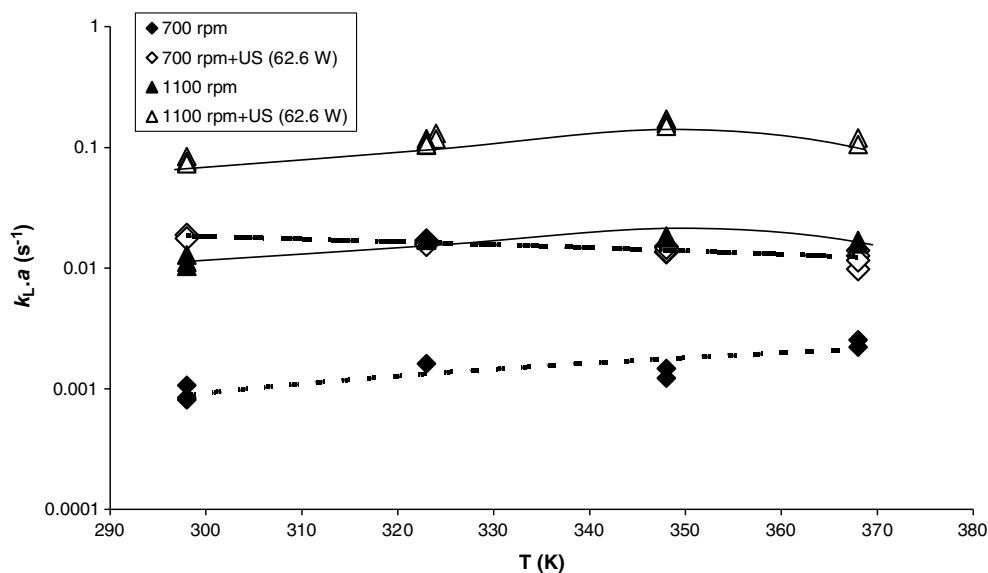

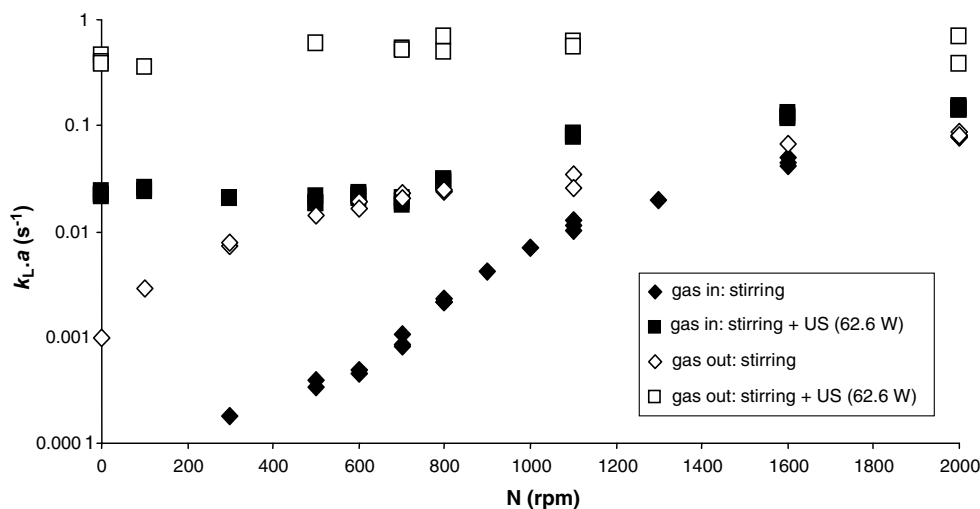**Fig. 7.** Effect of temperature on mass transfer at 11 bara.

Fig. 8. Comparison of kinetics of gassing in and gassing out (at 298 K, 10 bara).

mixing speed, $k_L \cdot a$ is equal to 0.5 ± 0.1 s. The experimental error on $k_L \cdot a$ is rather high (20%) because at time zero, pressure has to be purged down to atmospheric pressure, then reactor is closed as quickly as possible and sonication is started. All these operations require a few seconds, which cannot be neglected compared to the duration of a degassing run. Therefore, the measured $k_L \cdot a$ values are an underestimation of the real mass transfer coefficients of desorption experiments with sonication.

During adsorption and desorption runs in silent conditions the $k_L \cdot a$ values tend to the same limit when mixing speed is increased.

For absorption $k_L \cdot a$ sharply increases when N passes over the critical gas induction impeller speed (700 rpm), whereas for desorption, the evolution of mass transfer coefficient does not depend on impeller speed. So in desorption process, gas induction role is much reduced compared to absorption.

Energy consumption can be compared for degassing with sonication and with vigorous mixing: two experiments have been carried out with the same final pressure (0.35 barg), one under sonication at max power (62.6 W) and the other one only with stirrer at 2000 rpm (4.95 W). Time required for pressure to rise from 0 to 0.3 barg has been measured for both conditions: 12 s with ultrasound and 25 s with mechanical stirring.

So energy consumption by ultrasound is 751 J, whereas it is 619 J by mechanical stirring. So, even if sonication requires 17.6% energy more than mechanical stirring for desorption, required time is divided by two. As sonication also reduces the concentration in dissolved gas below solubility, it can be easily understood that degassing is a wide field of application of ultrasound.

5. Conclusion

Whereas the observed ultrasound effect on solubility is very low (below 12%), it has been proved that ultrasound greatly improves gas liquid mass transfer, especially below gas induction speed, this improvement being boosted by pressure. The effect of temperature is sensible but the effect of ultrasound depends mainly on the impeller speed. In typical conditions of organic synthesis: 323 K, 1100 rpm, 10 bara, $k_L \cdot a$ is multiplied by 11 when ultrasound is added to mechanical stirring.

The influence of sonication is much higher (about fivefold in same conditions) on gassing out kinetics than on gassing in, except at very low stirrer speed (below 500 rpm) because of very low values of $k_L \cdot a$ during absorption experiments. Moreover gassing out with ultrasound does not need mechanical stirring to be efficient and the presence of gas induced bubbles (over 700 rpm) does not influence desorption mass transfer at all. Sonication (62.6 W) is the fastest way to degas an oversaturated liquid, even if the required energy is 17.6% higher than under mechanical stirring at 2000 rpm (4.95 W), desorption is twice faster under sonication (62.6 W) than under mixing at 2000 rpm (4.95 W).

Finally the use of ultrasound in autoclave reactor for enhancing gas–liquid mass transfer is very efficient even in absence of gas induction (=without much agitation). Indeed the presence of bub-

bles induction is not necessary to see an impact of sonication on mass transfer, even more in their presence enhancement observed by ultrasound diminishes.

Ultrasound is thus a good tool to enhance gas–liquid mass transfer even at high pressure and temperature and even in absence of induced bubbles.

Note added in proof

This work has been partially presented at the 10th Congress of European Society of Sonochemistry in Hamburg (Germany, June 2006).

References

[1] T.J. Mason, Critical report on applied chemistry, in: T.J. Mason (Ed.), Chemistry with Ultrasound, vol. 28, Elsevier, Applied Science, 1990. published for the Society of Chemical Industry.
[2] Y. Chisti, Sonobioreactors: using ultrasound for enhanced microbial productivity, Trends Biotechnol. 21 (2003) 89–93.
[3] R. Bar, Ultrasound enhanced bioprocesses: cholesterol oxidation by *Rhodococcus erythropolis*, Biotechnol. Bioeng. 32 (1988) 655–663.
[4] J.V. Sinisterra, Application of ultrasound to biotechnology: an overview, Ultrasonics 30 (1992) 180–185.
[5] L.K. Weavers, M.R. Hoffmann, Sonolytic decomposition of ozone in aqueous solution: mass transfer effects, Environ. Sci. Technol. 32 (1998) 3941–3947.
[6] H. Zhang, L. Duan, D. Zhang, Absorption kinetics of ozone in water with ultrasonic radiation, Ultrason. Sonochem. 14 (2007) 552–556.
[7] Y. Adewuyi, Sonochemistry in environmental remediation. 1. Combinative and hybrid sonophotochemical oxidation processes for the treatment of pollutants in water, Environ. Sci. Technol. 39 (2005) 3409–3420.
[8] A. Kumar, P.R. Gogate, A.B. Pandit, H. Delmas, A.M. Wilhelm, Investigating mass transfer efficacy of sonochemical reactors, Ind. Eng. Chem. Res. 43 (2004) 1812–1819.
[9] O. Ayyildiz, P.R. Anderson, R.W. Peters, Laboratory batch experiments of the combined effects of ultrasound and air stripping in removing CCl₄ and 1,1,1-TCA from water, J. Hazard. Mater. B120 (2005) 149–156.
[10] O. Ayyildiz, R.W. Peters, P.R. Anderson, Sonolytic degradation of halogenated organic compounds in groundwater: mass transfer effects, Ultrason. Sonochem. 14 (2007) 163–172.
[11] N. Gondrexon, V. Renaudin, P. Boldo, Y. Gonthier, A. Bernis, C. Pétrier, Degassing effect and gas–liquid transfer in a high frequency sonochemical reactor, Chem. Eng. J. 66 (1997) 21–26.
[12] O.A. Kapustina, Degassing of liquids, in: L.D. Rosenberg (Ed.), Physical Principle of Ultrasonic Technology, vol. 1, Plenum press, New York, 1973.
[13] R. Sardeing, M. Poux, C. Xuereb, Les agitateurs auto-aspirants. Partie II: Dimensionnement et extrapolation, La houille blanche. 3 (2004) 75–88.
[14] M.M.P. Zieverink, M.T. Kreutzer, F. Kapteijn, J.A. Moulijn, Gas–liquid mass transfer in bench scale stirred tanks-fluid properties and critical impeller speed for gas induction, Ind. Eng. Chem. Res. 45 (2006) 4574–4581.
[15] A. Lekhal, R.V. Chaudhari, A.M. Wilhelm, H. Delmas, Gas–liquid mass transfer in gas–liquid–liquid dispersions, Chem. Eng. Sci. 52 (1997) 4069–4077.
[16] M. Jafari, J.S. Soltan Mohammadzadeh, Power consumption and onset speed for gas induction in a gas-induced contactor, Chem. Eng. J. 103 (2004) 1–5.
[17] A. Kapic, T.J. Heindel, Correlating gas–liquid mass transfer in a stirred-tank reactor, Chem. Eng. Res. Des. 84 (2006) 239–245.
[18] V. Schlüter, W.D. Deckwer, Gas–liquid mass transfer in stirred vessels, Chem. Eng. Sci. 47 (1992) 2357–2362.
[19] P.K. Chendke, H.S. Fogler, Effect of static pressure on the intensity and spectral distribution of the sonoluminescence of water, J. Phys. Chem. 87 (1983) 1644–1648.
[20] T.J. Mason, J.P. Lorimer, Sonochemistry: Theory, Application and Uses of Ultrasound in Chemistry, Ellis Horwood limited, 1988. p. 32.